Dynamics of fracture in dissipative systems

T. T. Rautiainen,[1] M. J. Alava,[2] and K. Kaski[1]
[1]*Laboratory of Computational Engineering, Helsinki University of Technology, P.O. Box 9400, FIN-02015 Espoo, Finland*
[2]*Laboratory of Physics, Helsinki University of Technology, P.O. Box 1100, FIN-02015 Espoo, Finland*
(Received 31 July 1997)

Dynamics of fracture in two-dimensional systems is studied with a dissipative network model by including the local relaxation of the force field via Maxwellian viscoelasticity. In addition to disorder the fundamentals of crack formation and propagation depend on the strength of dissipation compared to the loading rate. We investigate the dynamics of a single crack and the role of stress reduction at the crack tip when dissipation is increased. As a consequence, the crack starts to propagate slowly and it reaches terminal velocity later. If the relaxation of local forces is strong enough compared with crack velocity, crack arrest takes place. For a disordered system, the presence of strong dissipation in local dynamics is reflected as ductility and as an increase in the damage, accumulated during the fracture process. [S1063-651X(97)13511-5]

PACS number(s): 05.90.+m, 46.10.+z, 62.20.Mk, 83.50.By

I. INTRODUCTION

The development of failure in a medium has received a lot of attention due to its intrinsic technological importance [1]. The strength of a material depends on how small scale defects grow and get connected, and on the amount of disorder in it. The final breakdown occurs when one of the possibly many cracks has grown over a critical size. In addition to disorder many real materials, like fiber composites such as paper, polymers, and metals at high temperatures, display time-dependent properties. Such *viscoelastic* materials show creep and relaxation of applied stress and their response is highly sensitive to the loading rate [2]. The reason for viscoelastic response is, for example, in polymer melts believed to be the slow readjustment of macromolecules to the applied stress. It is similar to the dynamics of dislocations, that gives rise to plasticity in the stress-strain characteristics of metals.

The development of failure has been studied widely with discrete lattice models [3–6], in which the failure process takes place under adiabatic conditions. In this case the simulations are conducted in a way that corresponds to a slow rate of straining: the local stress field is allowed to readjust itself to the changes in the environment. Hence such quasistatic models involve no time scale, but a series of equilibrium states. In many real-life fracture problems, however, the material never reaches global elastic equilibrium, but the state of the system evolves dynamically. This involves, for example, the traveling of elastic waves in the system — caused by external impacts or propagating microcracks — which may result in some extra damage in the material.

In this paper we extend our previous study [7] of dynamic fracture in a simple time-dependent mesoscale system. We will concentrate on analyzing the interplay between disorder and dissipation. This paper is organized so that we first discuss the model. Then we present results of the single crack dynamics simulations, in which a small initial crack in the middle of otherwise homogeneous system has been introduced. Next we discuss the results of our simulations in a randomly bond-diluted disordered system. This part makes a more detailed study of the available parameter space than presented in our previous paper [7]. Finally we draw conclusions.

II. MODEL

In order to study the dynamics of fracture we have developed a phenomenological model that is simple enough for including viscoelasticity and allows simulations of relatively large systems. Initially our model is constructed to be a square mesh of size $L \times L$. Each site is assigned a unit mass, whose dynamical behavior will be monitored. These mass sites are not atomic but a site can be understood as the mass of a certain piece of material. Hence, the length scale of the model is mesoscopic rather than being microscopic as in conventional molecular dynamics models [8]. The mass sites are connected by nearest-neighbor bonds, as in quasistatic lattice models for fracture [3–6]. In our model the bottom row of masses is always kept fixed while the topmost row of masses is moved in unison and with a constant rate during tensile elongation in the y direction as denoted by $d\epsilon/dt$. In the x direction we apply periodic boundary conditions (see Fig. 1).

The elastic interaction strength of a bond ij between the

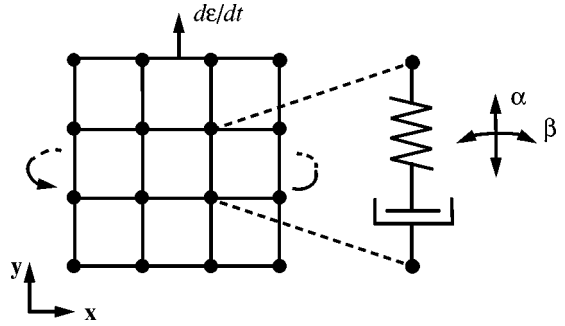

FIG. 1. Description of the model. Neighboring mass sites are coupled with dissipative Born springs, parametrized with tensile and bending stiffness α and β, respectively. The dynamics of the local bond forces are given by Eq. (2). A bond is missing with probability $(1-p)$.

nearest-neighbor sites i and j is described by the Born Hamiltonian [9]

$$H_{ij}=\frac{\alpha}{2}[(\vec{u}_i-\vec{u}_j)\cdot\vec{d}_{\parallel}]^2+\frac{\beta}{2}[(\vec{u}_i-\vec{u}_j)\cdot\vec{d}_{\perp}]^2, \qquad (1)$$

in which α and β are elastic coefficients related to the displacements parallel and perpendicular to the bond, $\vec{u}_j$ is the displacement vector of site j, and $\vec{d}_{\parallel,\perp}$ stands for the unit vector, either parallel or perpendicular to the vector connecting the sites in the undeformed mesh.

It should be noted that without an angular or bending part in the potential, the square mesh cannot describe deformations realistically, because it has directions in which shearing can happen without any cost of energy. The Born Hamiltonian is the simplest one in describing both the tensile and bending stiffness of a square mesh. Hence it is computationally less demanding than various other bond-bending Hamiltonians [5].

Since the Born Hamiltonian of Eq. (1) describes only the energetics of the system we have to include the choice of dynamics. This plays a crucial role in modeling fracture, because simultaneously at least one time scale is introduced, as in classical molecular dynamics simulations [8,10]. For the purpose of mimicking the local adjustment of the material structure to the stress we introduce a dissipation mechanism to the forces acting on mass sites. This is done through the classical Maxwellian viscoelasticity [2], which allows the description of relaxation and dissipation of elastic energy as a dynamical decay of the local forces. Hence the constitutive equation for the forces reads

$$\frac{\partial f_{ij}}{\partial t}=\frac{\partial f_H}{\partial t}-\frac{1}{\tau}f_{ij}, \qquad (2)$$

in which f_{ij} is the dynamical force between neighboring sites i and j, and f_H is the elastic or reversible force derived from the Born Hamiltonian. τ is a phenomenological dissipation constant, which sets the internal time scale for the relaxation of the forces. Thus our choice of local dynamics is equivalent to a Born spring with tensile and bending stiffness in series with a viscous dashpot. This can be seen as a general Maxwellian viscoelastic element describing a bond as depicted in Fig. 1.

There are a number of ways to introduce disorder into the system. For example, the fracture limit or some of the bond parameters (α, β, τ) could be locally distributed. In this study we have chosen the disorder to be quenched bond-disorder, i.e., a fraction of bonds has been removed at random with probability $(1-p)$. When $p=0.5$ there is already a percolating path through the system. For $p>0.5$ under loading, a fracture path grows dynamically through the system as a result of bonds rupturing at the given fracture limit.

The criterion for bond rupture can be based either on the amount of stress or strain in it. Here we have taken the latter alternative by defining the bond rupture to occur when its tensile elongation exceeds 1%, i.e., we denote $\epsilon_f=0.01$. This fracture condition can be compared with that used by Sornette and Vanneste (SV), whose lattice model [11] is based on the rupture of fuse elements, when the local temperature exceeds a critical value. In their study the continuously changing temperature field, controlled by the individual fuse currents, is analogous to plastic deformation. However, in our model the local strain is directly responsible for the onset of fracture. In both cases, the instantaneously high stresses, or currents in the SV model, do not necessarily break the bond, but the memory from previous deformations — included in the bond length, or fuse temperature in the SV model — may cause the rupture at low local stress levels. In interpreting our simulations, it should also be remembered that the redistribution of internal stresses occurs with a finite speed. This is in contrast to the quasistatic models.

In the simulations the normalized strain rate per bond is chosen to be $d\epsilon/dt=2.5\times10^{-4}$ (in most cases) or 2.5×10^{-5}. Hence, the topmost row of the system is moved with the rate $L\times d\epsilon/dt$. For a given strain rate $(d\epsilon/dt)$, the dissipation constant τ and the strength of elastic interactions (α, β) determine the time scales of our model dynamics. In addition to these time scales the fracture limit determines a macroscopic time scale, which is the average time for the failure to be of the order $\epsilon_f/(d\epsilon/dt)$. Compared to the linear dependence between local stress and strain in models for elastic materials, our choice for the constitutive relation implies that the local stress depends not only on the present strain, but on the whole preceding strain history.

The time scales of the system, especially the harmonic ones (related to α and β), require the time step of integration δt in Eq. (2) to be sufficiently small. In addition, the requirement in the simulations to allow only one bond at a time to break sets another limitation to the allowed time step. In order to find a fast and sufficiently accurate integration method we tested two algorithms, the simple Euler and the original Verlet [8], using $\delta t=0.001$. Both of these algorithms gave indistinguishable results for the same initial configuration. Also we varied the time step of the Euler algorithm between 0.004 and 0.0005 without seeing any significant change in the results.

It should be borne in mind that the introduction of the constant strain rate at time $t=0$ — also the time for starting the integration of Eq. (2) — will initially generate a shock wave to the system. The amplitude of this shock wave shows a dependence on the constant strain rate. For $d\epsilon/dt=2.5\times10^{-4}$ this amplitude was found to be less than 0.1% of the initial bond length. The effect of the initial shock wave diminishes if the constant strain is decreased or the strain rate increases gradually from zero to the constant value. In disordered systems, however, the coherence of these shock wave tends to be lost.

Finally some remarks about the length and time scales of our model are in order. First we note that our model does not have a real physical length scale, rather we have considered a vague counterpart. A mesoscopic scale was chosen to describe materials that show (strong) disorder in terms of density distribution or are otherwise difficult to model in microscopic scale. An example of such material is paper that shows density variations ranging from submillimeter scale up to a few millimeters. Now if we were to carry out simulations with a denser mesoscale mesh in the same physical system, the mass of each site and the elastic coefficients should be scaled such that the macroscopic properties like Young's modulus and the total mass of the system remain unchanged. However, due to the fact that we are lacking

experimental observations of the time scale of the mesoscopic viscoelastic effects, the question of how the phenomenological dissipation constant should be scaled remains unsolved. Then instead of checking mesh convergence we have checked the finite size effects by changing the system size from mostly studied $L=100$ up to $L=200$, but without changing the mass, elastic coefficients, and dissipation constant. The results were found to be the same. All in all, we expect our simple model to describe some salient features of real systems.

III. RESULTS

A. Single crack dynamics

In order to characterize the role of dissipation in the crack propagation process, we first investigate the behavior of a single crack in an otherwise homogeneous sample. Somewhat similar studies have been made by Sieradzki *et al.* [12] and Furukawa [13]. However, our system is not intended to mimic an infinite sample, and hence the finite size effects are expected to influence crack propagation by changing the stress enhancement around the crack tip [21]. Initially we introduce a small crack in which two adjacent bonds parallel to the external loading are removed from the middle of the sample. This serves as the seed of crack propagation under sufficient external straining. The velocity of the crack tip is investigated under constant strain rate by varying the dissipation (τ) and the bending stiffness of the bonds (β).

In Fig. 2 we show snapshots of stress distributions in the sample during crack propagation. In weakly dissipative systems, the abrupt loading procedure causes a shock wave, which is seen as a background ripple. Increasing the amount of dissipation makes the ripple disappear. A much more spectacular feature is seen when the rupture of an individual bond releases the constraining force at that particular point. As a result the neighboring bonds experience increased stress, which spreads out of the damaged area at most with the longitudinal speed of sound, i.e., $v_s \simeq \sqrt{\alpha}$ (with the proper choice of units). In this model the shape of the relaxing stress field is determined by the ratio between the tensile stiffness (α) and bending stiffness (β). Due to the finite sample size, the stress waves of bond ruptures reflect from the upper and lower sample boundaries, yielding an interference pattern. This is also how the crack may interact with itself due to a finite sample size.

Knowing the speed of sound (v_s) and the crack velocity (v_{crack}) we can estimate the time for the reflected shock wave to interact with the propagating crack tip. If measured from the rupture of the bond, the time required for the wave to reach the crack tip is $t_1 > 2\Delta y/\sqrt{\alpha}$, where Δy is the shortest distance from the sample boundary to the crack. Thus, by t_1 the crack tip has moved a distance $\Delta x \sim v_{\mathrm{crack}} t_1 \sim 2 v_{\mathrm{crack}} \Delta y/\sqrt{\alpha}$. Then at the elastic limit, we obtain for the crack tip velocity a $\sqrt{\beta}$ dependence (see the details in the Appendix). The same dependence is seen for the saturated value of the crack velocity in Fig. 3. Thus we conclude that in case of small or moderate dissipation ($\tau \gtrsim 10$) the reflected shock wave may affect the crack propagation, provided that the α/β ratio is large, or the distance Δy is small. The traveling shock wave can enhance the crack growth by bringing the bond in front of the straight propagating crack earlier to its rupture limit than without it.

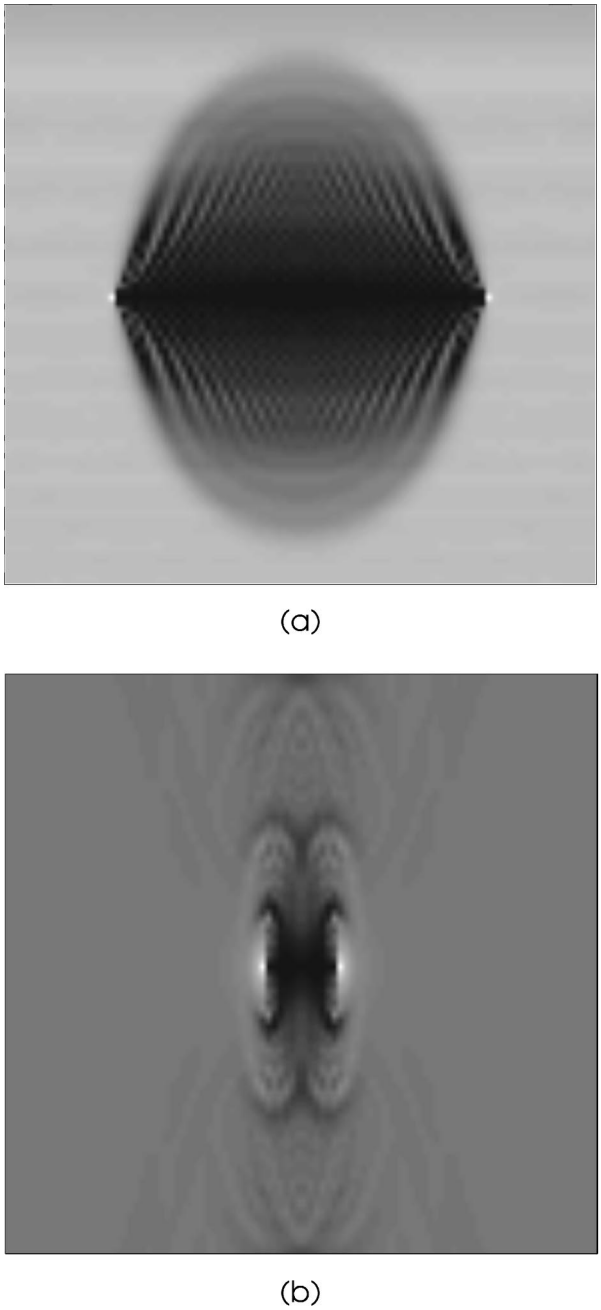

FIG. 2. Snapshots of the stress distributions in bonds parallel to the loading. (a) $\tau=100$, $\beta=250$, (b) $\tau=10$, $\beta=50$. In both the figures $L=100$, $d\epsilon/dt=2.5\times10^{-4}$, and $\alpha=500$.

In weakly dissipative systems ($\tau=100$), the crack tip velocity reaches its terminal value rapidly, as depicted in Fig. 3. This occurs especially for large values of β, which accounts for increased bending stiffness between neighboring mass sites. With increasing dissipation, however, the effect of relaxation becomes noticeable at the beginning of crack propagation. Due to inertia the crack tip starts to move slowly, and it reaches the terminal velocity later than in weakly dissipative samples. In addition, the terminal velocity is slightly decreased (about 10%) compared to the system with $\tau=100$. In Fig. 3 we also show a striking case of very strong dissipation ($\tau=1.5$). The slow startup of crack propa-

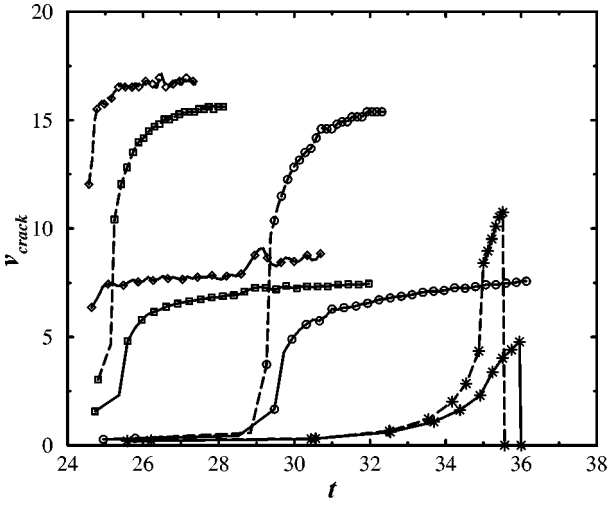

FIG. 3. Crack tip velocity vs time. $\alpha=500$ and $\beta=50$ (solid lines) and $\beta=250$ (dashed lines). The symbols are assigned with different degrees of dissipation: *, $\tau=1.5$; ○, $\tau=5$; □, $\tau=10$; ◇, $\tau=100$.

gation is even more prominent and the crack tip velocity does not reach a terminal velocity but drops to zero. Therefore, we can separate three regimes in the $v_{\mathrm{crack}}(t)$ curves of Fig. 3. For small and moderate dissipation ($\tau \geqslant 10$) there is the regime of short initial transient and fast saturation to a β-dependent terminal velocity. Then for strong dissipation ($\tau \leqslant 5$) there is the regime of long initial transient and slower saturation to a terminal velocity. Finally, for very strong dissipation ($\tau \leqslant 1.5$) there is a regime of very long initial transient, ending up in a *crack arrest*.

The effect of dissipation on the local forces in the system is depicted in Fig. 4, which shows stress profiles ahead of the propagating crack tip. It is evident that increasing the amount of dissipation will decrease the stress values dramatically. A weakly or moderately dissipative system [Fig. 4(a), $\tau=10$] exhibits a dynamic stress profile, in which the magnitude of the maximum stress at the crack tip shows a fast initial increase and then it decays slowly throughout the propagation

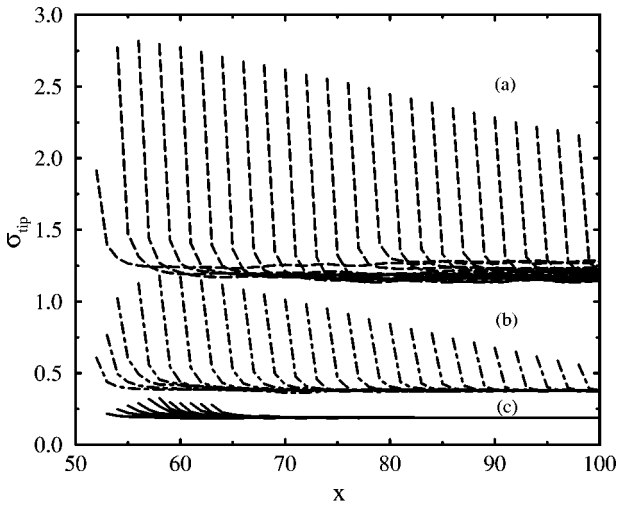

FIG. 4. Stress profiles ahead of the propagating crack tip immediately before the next bond rupture. $\alpha=500$ and $\beta=250$. (a) $\tau=10$, (b) $\tau=3$, (c) $\tau=1.5$. The x coordinate is defined as in Fig. 1.

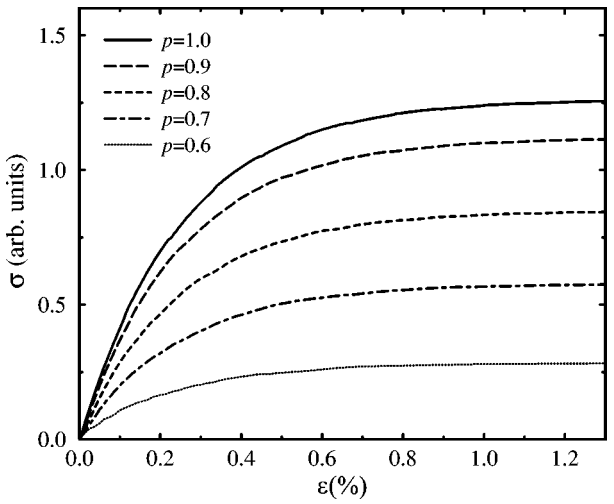

FIG. 5. Stress-strain curves for various degrees of dilution, p = 1.0, 0.9, 0.8, 0.7, and 0.6, with $L=100$, $\alpha=500$, $\beta=250$, and $\tau=10$.

until the final failure. This behavior corresponds to the regime of short initial transient and fast saturation to a terminal crack velocity. For strong dissipation [Fig. 4(b), $\tau=3$] the initial increase in the stress maximum is gradual, followed by a fast decay until the final failure. This behavior corresponds to the intermediate regime of long initial transient and slower saturation to a terminal crack velocity. Finally, for very strong dissipation [Fig. 4(c), $\tau=1.5$] the stress maximum grows again slowly to a small value then decaying until the point of crack arrest. Now the stress profile has become flat showing only a very minor deviation from the background stress. This small stress makes further bond elongation at the crack tip very slow at best, causing bond ruptures to stop or occur elsewhere in the system. If we increase the dissipation even further ($\tau<1.5$), the stress enhancement at the crack tip becomes insufficient to cause even a single bond rupture. Thus we conclude that very strong dissipation makes the system ductile.

In recent experiments [14] and simulations [15,16] crack tip branching has been seen. These are caused by another mechanism of changing stress field distribution which our model as such cannot repeat. This is due to the initial mesh geometry, loading direction, and the chosen fracture criterion. In our model with the load being along the principal mesh direction it is always most beneficial for the crack to propagate straight through the system along the other principal mesh direction. However, crack branching is seen to occur in such mesh geometries as triangular or hexagonal meshes but also in square meshes that are loaded in a direction different from the principal mesh direction, e.g., along the mesh diagonal. A more detailed account of crack branching using the same computer model as we have done but in a triangular lattice has been presented by Heino and Kaski [17–19], and therefore further discussions are omitted here.

B. Disordered system

Now we move over to study disordered systems with random bond dilution, below the percolation threshold, i.e., $p>0.5$. In Fig. 5 we present the loading characteristics of moderately dissipative systems ($\tau=10$) for various degrees

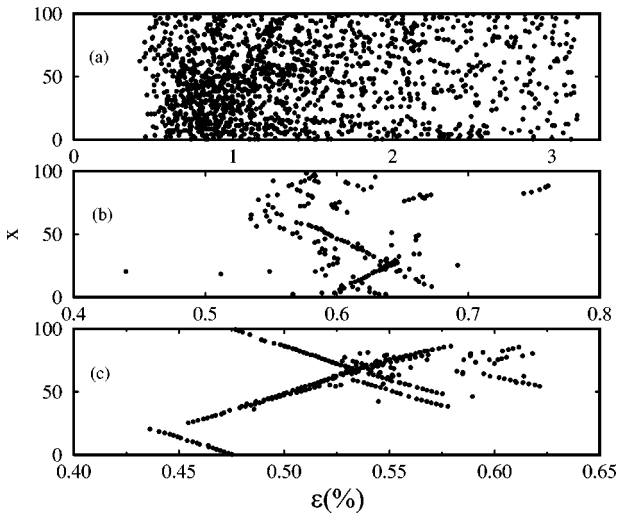

FIG. 6. The dynamical development of cut bonds perpendicular to the external strain. $\alpha=500$, $\beta=250$ and (a) $\tau=100$, (b) $\tau=10$, (c) $\tau=1$. $L=100$ and $p=0.9$, the initial disorder in the system being identical in all these cases.

of disorder before final fracture. The general features of the stress-strain behavior are of a material displaying Maxwellian viscoelasticity. Under steadily increasing strain there is an initial region that corresponds to ideal elasticity crossing over to a viscous phase, with a final state of constant stress.

For strong dissipation, internal stresses relax rapidly, and the system under further straining settles down to a low stress level. On the other hand, for negligible dissipation, the behavior of a system resembles that of ideal Born springs. The role of dissipation can be described through the product $\tau\, d\epsilon/dt$, which serves as a measure of elastic properties of a system [23]. It also determines the steady-state stress, which is achieved with sufficient straining. In the limit of vanishing strain rate and dissipation, the ensuing force-elongation characteristics turn out to be equal with those of a corresponding adiabatic model [6].

The reduction in stress enhancement with increasing dissipation described by the single crack case (Fig. 4) is clearly reflected on the fracture behavior of disordered systems. For finite strain rates, different regimes are observed in the fracture process. Their characteristics for small amount of disorder ($p=0.9$) are demonstrated in Fig. 6, which shows how individual fracture events evolve in the direction perpendicular to the external strain. For negligible dissipation [$\tau=100$, Fig. 6(a)] fracture is found to be dependent on the loading procedure. The initial shock wave, caused by the abrupt application of constant strain rate, travels back and forth practically without decaying and may break individual bonds here and there in an uncorrelated manner. Due to the lack of dissipation, and especially increased stress enhancement, these microruptures, together with the pre-existing disorder, soon start to correlate. When one of the cracks starts to dominate, the system suffers rapidly a macroscopic breakdown. This can be interpreted as the crack propagation phase. In general, at finite strain rates with very small dissipation, there may exist competing microcracks, which have nucleated from several defects — not only from the most critical one [20], as is common in models of brittle fracture with fixed disorder. The microcracks exhibit correlated growth and can eventually coalesce. Thus the fracture process depends on the dynamical evolution of individual mass sites, not only on the initial disorder.

In Fig. 6(c) we show the fracture behavior in the opposite extreme of very strong dissipation, i.e., $\tau=1$. Dissipation damps effectively all the disturbances in the system, and the shock wave introduced at the beginning of loading has no effect on the fracture behavior. As already seen in the case of single crack dynamics, cracks start to propagate very slowly — if at all — from initial defects. Similarly with the case of single crack dynamics (see Fig. 4) the stress enhancement at the crack tip is strongly reduced compared to the weakly or moderately dissipative system. There is practically no potential energy stored in the bonds, and an individual rupture does not necessarily cause the next bond rupture to take place close to the current one. The interactions between neighboring mass sites diminish and the local dynamics becomes more and more independent of the dynamics of the surroundings. The lack of crack tip related stress enhancement makes the system very ductile. As a result, very strongly dissipative systems evolve towards the macroscopic breakdown via numerous microruptures in an uncorrelated fashion, as can be seen in Fig. 6(c). In contrast to the weakly dissipative system this system is capable of withstanding a considerable amount of external strain. Eventually, this drives the system far from its initial mesh geometry to a drastically deformed final configuration, from which it is unable to return to its original form. In real materials this phenomenon can be interpreted as permanent plastic deformation, which in our model is captured by the dissipative nonrecoverable response of the dashpot elements. Note that if the strain rate is sufficiently high, the strain distribution in the system shows a bias towards the strained edge. Thus in spite of the initial disorder, the bonds near the strained edge are likely to meet the fracture condition first.

Between the above extremes lies the regime of moderate dissipation [$\tau=10$, Fig. 6(b)] which shows features of both the weakly and very strongly dissipative systems. For small amount of strain, i.e., early in the straining history, uncorrelated bond ruptures appear here and there. When the straining increases bond ruptures show once again correlation and several microcracks tend to grow. This behavior of microcrack nucleation is reminiscent of ductility in a strongly dissipative system. In Fig. 6(b) we also observe several local crack arrests, most likely due to dissipation.

In Fig. 7 we show the number of cut bonds as a function of increasing strain for various amounts of disorder [22]. In the main figure of the present paper the cases of strong ($\tau=5$) and very strong ($\tau=1$) dissipation are displayed, while the inset shows the behavior of a very weakly dissipative system ($\tau=100$). In these curves the end points indicate the final fracture. As a general observation we can state that when disorder increases (p decreases), the amount of damage the system can withstand decreases rapidly. Also the more dissipative the system is, the more damage it can withstand before final fracture, i.e., the system shows increased ductility for increased dissipation.

In addition, we see that in a weakly disordered system ($p=0.8-0.9$) the proportion of ruptured bonds first grows rapidly. Then the accumulation of damage becomes slower, and the system is able to accommodate additional straining.

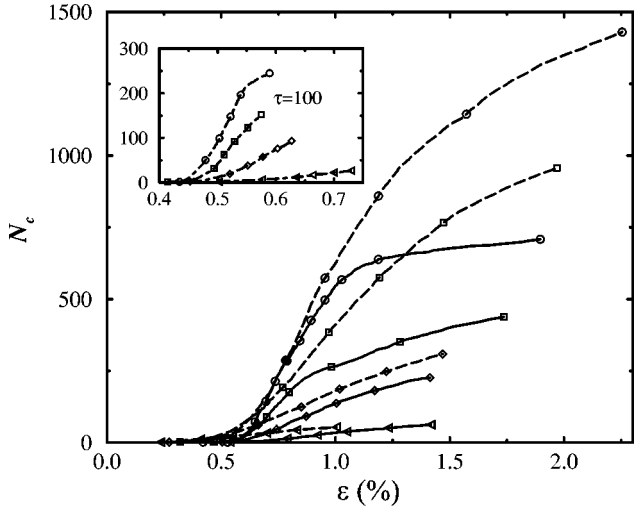

FIG. 7. Time development of the number of cut bonds N_c in 100×100 systems with $d\epsilon/dt=2.5\times10^{-4}$, for two values of dissipation ($\tau=1$ and $\tau=5$) and increasing disorder ($p=0.9$, 0.8, 0.7, and 0.6). $\alpha=500$ and $\beta=250$. The inset illustrates the fracture behavior with $\tau=100$. The end points of the curves indicate the final fracture. The curves are averaged over several simulation runs.

However, in strongly disordered systems ($p=0.6-0.7$) this tendency is lost. From the inset of Fig. 7 we see that a weakly dissipative but strongly disordered system is able to withstand more strain than a weakly disordered one. For the system with strong or very strong dissipation, this behavior is reversed: a weakly disordered system bears straining most since the individual bond ruptures do not correlate [cf. Fig 6(c)].

In Fig. 8 we show configurations of a system with small disorder ($p=0.9$) after final failure for three different values of dissipation. The initially removed bonds are exactly the same in all these cases, so that differences arise only from variations in dissipation. Under loading, the system with $\tau=1$ suffers from damage occurring all over the system due to microruptures being uncorrelated. Separately propagating cracks are hardly distinguishable, as was observed already in Fig. 6(c). The amount of damage is clearly diminished with decreasing dissipation in Figs. 6(b) and 6(a), where ruptures are concentrated in cracks. If p is close to unity, the number of removed bonds is very few and scattered. Then in weakly dissipative systems the dynamically generated fracture paths are rather straight, especially if the α/β ratio is large. If the disorder is increased, i.e., p decreases, the picture emerging from our model follows that seen in adiabatic simulations: the wandering of the final crack becomes more erratic, as the removed bonds contribute significantly to the final fracture path and the breakings of distant, individual bonds are sufficient to bring about the final fracture. Decreasing β is attributable to the diminished interactions between the rows of bonds, which also enhances the wandering of the crack tip. In addition, the initial disorder in the system provides random points of crack branchings.

We have also studied the behavior of the system with smaller strain rate $d\epsilon/dt=2.5\times10^{-5}$. Simultaneously the value of τ was scaled in order to keep the product $\tau\, d\epsilon/dt$ unchanged. In this case the differences between fracture regimes diminish. The dynamics of fracture becomes less sensitive to varying degree of dissipation, especially in systems with moderate or weak dissipation. At slow strain rates, it is easier for the system to follow changes due to loading. Hence, in weakly dissipative systems, the local strains adjust

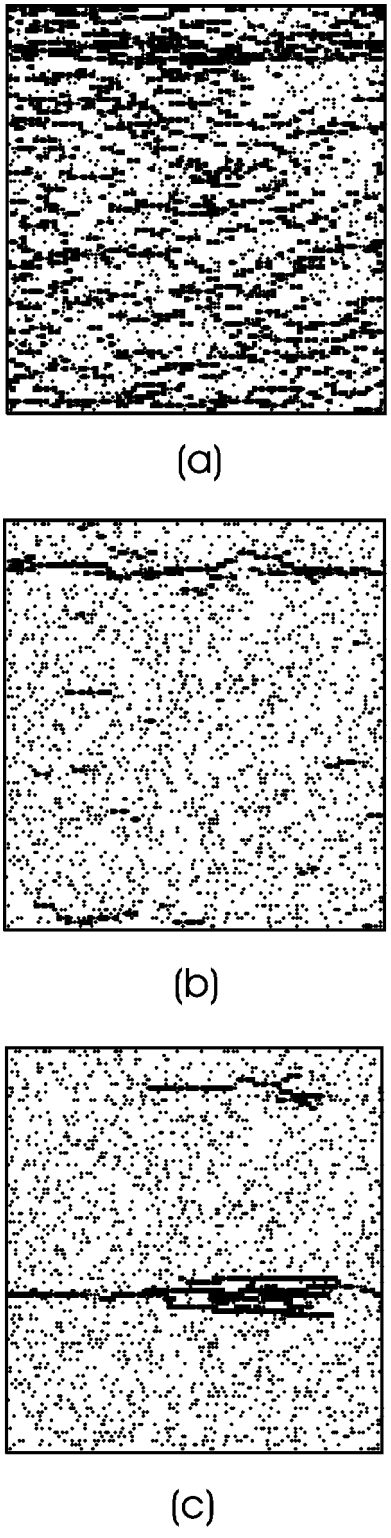

FIG. 8. Final configurations after breakdown in 100×100 systems with $p=0.9$. The filled circles correspond to initially randomly removed bonds while the squares are loading induced cut bonds. (a) $\tau=1$, (b) $\tau=10$, and (c) $\tau=100$. The initial disorder in the system is exactly identical for all values of τ.

rapidly and the local stresses correspond better to the external loading configuration. This inhibits multiple cracks from growing. In addition, a weakly dissipative system is not so strongly affected by the loading procedure, nor does it any longer support several independent simultaneously propagating cracks. The fracture shows very brittle characteristics, as is typical for elastic systems under adiabatic loading conditions. When strain rate is reduced to $\frac{1}{10}$, a system with strong dissipation, however, does not exhibit a drastic change in fracture characteristics. In the limit of vanishing strain rate, the adiabatic behavior of quasistatic lattice models [6,24,25] is encountered.

Apart from using the same set of parameters as in Fig. 6 we have also studied the system with lower bending stiffness ($\beta=50$). We find the system to be more ductile, i.e., withstanding more strain, than the system with higher bending stiffness ($\beta=250$). Otherwise these systems behave similarly. It is also seen that the number of simultaneously propagating microcracks grows, which is attributable to the diminished interactions between the rows of bonds. Thus, concerning ductility and elastic stiffness of the systems, the α/β ratio has a similar effect on mechanical properties as dissipation: increased ductility corresponds to a decrease in the capability of the system to store elastic energy.

IV. CONCLUSIONS

We have investigated fracture dynamics in systems with varying degree of dissipation and disorder. In the single crack study the effect of dissipation on the crack propagation process was most striking at the beginning of the crack propagation phase, whereas in the end of this phase the terminal velocity exhibited $\sqrt{\beta}$ dependence. The slow startup of crack propagation was attributable to the increased dissipation, which eventually stopped or completely inhibited the crack growth. In disordered systems, the strong dissipation was reflected in the slow crack nucleation and uncorrelated microruptures, leading to very ductile characteristics. On the other hand, very brittle behavior was encountered in nearly elastic and weakly disordered systems, in which propagating cracks could clearly be distinguished, and macroscopic failure occurred soon once one of the cracks started to dominate. Between these extremes lies a fracture regime, which showed features of both the ductile and brittle characteristics: clearly correlated crack growth resembling the weakly dissipative characteristics, but also crack arrest due to presence of dissipation. However, with increasing disorder, these differences become less pronounced. In the limit of slow dynamics, the fracture characteristics of our model approach those of typical adiabatic models. The differences are due to the finite strain rate and the nonlinear dissipative response of the system.

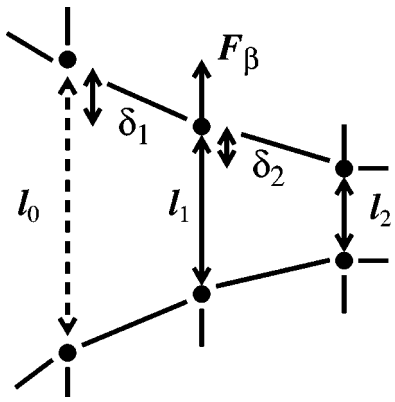

FIG. 9. Configurational model of a crack tip.

ACKNOWLEDGMENTS

This work is in part supported by the Academy of Finland through the MATRA program and the Technology Development Center of Finland.

APPENDIX

Let us consider a configurational model of a crack tip (cf. Ref. [13]), in which for simplicity the bonds are assumed to be purely elastic Born-type springs; see Fig 9. The leftmost bond is supposed to represent the crack tip, which has just reached the fracture threshold. Then its length is $l_0=1+\epsilon_f$, and the next two intact bonds ahead of the crack tip have lengths $l_1=1+\epsilon_1$ and $l_2=1+\epsilon_2$, respectively. For these strain values the following holds: $\epsilon_2<\epsilon_1<\epsilon_f$. Due to bond rotation, the mass sites of the crack tip ''feel'' in the y direction a net force $F_\beta=\beta(\delta_1-\delta_2)$, in which $\delta_1=(\epsilon_f-\epsilon_1)/2$ and $\delta_2=(\epsilon_1-\epsilon_2)/2$ (only the upper half of the otherwise symmetric configurational model is considered). As a consequence of the acceleration of the mass site (with mass m), the first intact bond is expected to reach the fracture threshold condition in time $t=\sqrt{2\delta_1 m/F_\beta}$. This gives us the following estimate for the crack tip velocity: $v_{\mathrm{crack}}=k\sqrt{\beta/m}$, where k includes the strain field geometry via ϵ_1, ϵ_2, and ϵ_f. Although we have assumed idealized steady-state conditions and neglected all initial velocities in this analysis, $v_{\mathrm{crack}}\sim\sqrt{\beta}$ is revealed.

[1] B. Lawn, *Fracture of Brittle Solids*, 2nd ed. (Cambridge University Press, Cambridge, England, 1993).
[2] W. Flügge, *Viscoelasticity*, 2nd ed. (Springer-Verlag, Berlin, 1975).
[3] H.J. Herrmann and S. Roux, *Statistical Models for the Fracture of Disordered Media* (North-Holland, Amsterdam, 1990).
[4] M. Sahimi, Physica A **186**, 160 (1992).
[5] M. Sahimi and S. Arbabi, Phys. Rev. B **47**, 703 (1993).
[6] G.N. Hassold and D.J. Srolowitz, Phys. Rev. B **39**, 9273 (1989).
[7] T.T. Rautiainen, M.J. Alava, and K. Kaski, Phys. Rev. E **51**, R2727 (1995).
[8] M.P. Allen and D.J. Tildesley, *Computer Simulation of Liquids* (Clarendon Press, Oxford, 1990).
[9] M. Born and K. Huang, *Dynamical Theory of Crystal Lattices* (Oxford University Press, London, 1954).

[10] N.J. Wagner, B.L. Holian, and A.F. Voter, Phys. Rev. A **45**, 8457 (1992); Z.-G. Wang *et al.*, Phys. Rev. B **44**, 378 (1991); W. Brostow and J. Kubat, *ibid.* **47**, 7659 (1993); J. Gao and J.H. Weiner, Macromolecules **25**, 1348 (1992).
[11] D. Sornette and C. Vanneste, Phys. Rev. Lett. **68**, 612 (1992).
[12] K. Sieradzki, G.J. Dienes, A. Paskin, and B. Massoumzadeh, Acta Metall. **3**, 651 (1988).
[13] H. Furukawa, Prog. Theor. Phys. **90**, 949 (1993).
[14] E. Sharon, S.P. Gross, and J. Fineberg, Phys. Rev. Lett. **74**, 5096 (1995).
[15] M. Marder and X. Liu, Phys. Rev. Lett. **71**, 2417 (1993).
[16] F.F. Abraham, D. Brodbeck, R.A. Rafey, and W.E. Rudge, Phys. Rev. Lett. **73**, 272 (1994).
[17] P. Heino and K. Kaski, Phys. Rev. B **54**, 6150 (1996).
[18] K. Kaski and P. Heino, J. Molecular Liquids **71**, 225 (1997).
[19] P. Heino and K. Kaski, Phys. Rev. E **56**, 4364 (1997).
[20] P.M. Duxbury, P.D. Beale, and P.L. Leath, Phys. Rev. Lett. **57**, 1052 (1986).
[21] C. Vanneste, A. Gilabert, and D. Sornette, J. Phys. A **23**, 3591 (1990).
[22] Because of a small programming error results shown in the corresponding figure (Fig. 3) of our earlier paper [7] were correct qualitatively but not quantitatively.
[23] By increasing the strain rate the response of, for example, polymeric material exhibits more elastic characteristics; see H.-H. Kausch, *Polymer Fracture* (Springer-Verlag, Berlin, 1987).
[24] The time dependence of failed bonds in simulations of brittle polymers shows similar features. See D. Blonski and W. Brostow, J. Chem. Phys. **95**, 2890 (1991).
[25] M.J. Alava and R.K. Ritala, J. Phys.: Condens. Matter **2**, 6093 (1990).